2018 21st International Conference on Intelligent Transportation Systems (ITSC)
Maui, Hawaii, USA, November 4-7, 2018

A Control Strategy Combined Thermostat Control with DC-Link Voltage Control for Series Hybrid Electric Vehicles

Can Luo
State Key Laboratory for Management and Control of Complex Systems, Institute of Automation, Chinese Academy of Sciences, Beijing, China
Qingdao Academy of Intelligent Industries
Qingdao, China
can.luo@ia.ac.cn

Zhen Shen
State Key Laboratory for Management and Control of Complex Systems, Institute of Automation, Chinese Academy of Sciences, Beijing, China
Cloud Computing Center, Chinese Academy of Sciences,
Dongguan, China
zhen.shen@ia.ac.cn

Simos Evangelou
(Corrensponding Author)
Department of Electrical and Electronic Engineering, Imperial College London
London, UK
s.evangelou@imperial.ac.uk

Gang Xiong
Beijing Engineering Research Center of Intelligent Systems and Technology, Institute of Automation, Chinese Academy of Sciences, Beijing, China
gang.xiong@ia.ac.cn

Xiao Wang
Qingdao Academy of Intelligent Industries
Qingdao, China
x.wang@ia.ac.cn

Yisheng Lv
Qingdao Academy of Intelligent Industries
Qingdao, China
yisheng.lv@ia.ac.cn

Xisong Dong
Qingdao Academy of Intelligent Industries
Qingdao, China
xisong.dong@ia.ac.cn

Fenghua Zhu
Beijing Engineering Research Center of Intelligent Systems and Technology, Institute of Automation, Chinese Academy of Sciences, Beijing, China
fenghua.zhu@ia.ac.cn

Fei-Yue Wang
State Key Laboratory for Management and Control of Complex Systems, Institute of Automation, Chinese Academy of Sciences, Beijing, China
feiyue.wang@ia.ac.cn

***Abstract*—In this paper, we introduce the combination of thermostat control strategy (TCS) and DC-link voltage control strategy to improve fuel economy for series hybrid electric vehicles (HEVs). The main method is tuning essential parameters, including a parameter under DC-link voltage control and a selected constant as an important judgement condition of charging operation modes under TCS. The minimum mass points of equivalent fuel consumption (EFC) corresponding to a series of variables are marked for worldwide harmonized light vehicles test procedure (WLTP). By analysis and verification, the fuel economy of series HEVs with WLTP performs better with the combination control schemes than individual control scheme, so this scheme proves very effective for series HEVs driving in an urban environment.**

Keywords—series hybrid electric vehicles; thermostat control Strategy; DC-link voltage control; tuning; equivalent fuel consumption

I. INTRODUCTION

A. Background

The development history of vehicle is over 100 years. The vehicle has become an important symbol of modern civilization. However, there are more than 100 kinds of pollutants in automobile exhaust [1] and the vehicle causes the noise pollution, traffic accidents, shortage of oil resources, and other serious challenges. Electric vehicle (EV) has a lot advantages for environment, energy and technical concerns, so governments pay more attention to development of EV. HEV is a suitable transition between pure electric vehicles and traditional vehicles.

In the past half century, control systems have been developed to run various industrial devices [2-5]. Control systems are also essential for vehicles, which can improve driving performance to satisfy increasing efficiency requirement [6-9]. TCS and DC-link voltage control strategy are two kinds of control strategies for HEV and control different variables of different modules respectively. TCS mainly influences operative modes of primary source and secondary source, while DC-link voltage control mainly controls DC-link voltage to influence battery efficiency. Thus, it is possible to obtain better performance by combining the two strategies together.

B. Series Hybrid Electric Vehicles

Series HEV is a kind of HEVs. For series HEV, the series drivetrains are the simplest hybrid configuration[10]. The powertrain of series HEV includes: the primary source (PS), the secondary source (SS) and the propulsion load (PL). The diagram of the series HEV is given in Fig.1.

As power sources, the PS and SS provide power for PL. The relationships of them are as follows：

$$P_{PS} + P_{SS} = P_{PL} \tag{1}$$

P_{PL} represents the load power of PL. P_{SS} represents the power of SS. P_{PS} represents the output power of PS.

This work is supported in part by National Natural Science Foundation of China under Grants 61773382, 61773381, 61533019, 91720000，61806198，71702182，61702519; Chinese Guangdong's S&T projects 2017B090912001, 2016B090910001;Beijing Municipal Science & Technology Commission (Z181100008918007) 2016 S&T Benefiting Special Project (No.16-6-2-62-nsh) of Qingdao Achievements Transformation Program; Dongguan's Innovation Talents Project (Gang Xiong)

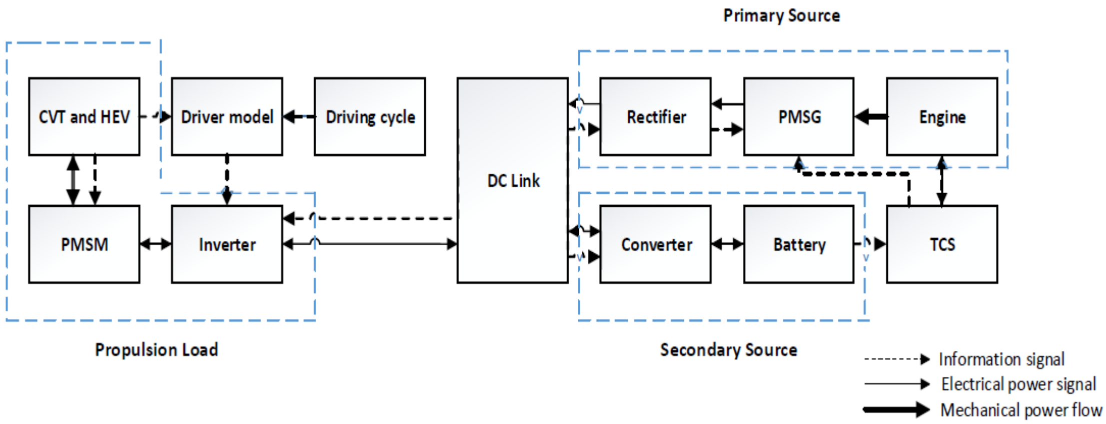

Fig. 2. The diagram of series HEV powertrain

Propulsion Load: PL mainly includes permanent magnet synchronous motor (PMSM) and continuously variable transmission (CVT). CVT links the wheel of the vehicle and the motor. The PMSM connects the DC link of the powertrain by an inverter. The inverter is bi-directional, that is, when braking happens, it works as a rectifier. The inverter links the motor and the DC bus. The condition losses and switching losses are essential for the inverter [11][12].

Primary Source: The primary source of HEV includes permanent magnet synchronous generator (PMSG), internal combustion engine (ICE) and rectifier. PMSG connects ICE. ICE transforms chemical energy to mechanical energy, while PMSG converts the mechanical energy to electrical energy.

Secondary Source: Second source of HEV mainly includes battery and converter. There are two essential parameters for DAB converter: the ratio of voltage conversion (d) and the phase shift (φ) between the primary and secondary signals of switch gating. The expression of d is as follows:

$$d=\frac{v_0}{nv_i}. \tag{2}$$

v_0 and v_i represent the output and input voltages of the DAB converter respectively. n represents the ratio of transformer [13]. φ represents phase shift between the primary and secondary signals of switch gating. The value of φ can show the power flow direction. The relationship expression about φ and average power of DAB converter is given [13] as follows:

$$P_{avg} = v_i v_0 \varphi(\pi - \varphi)/2n\pi^2 Lf \tag{3}$$

The symbol f represents the frequency of DAB converter switching. L represents leakage inductance of the DAB converter. There are two modes for the DAB converter: boost mode (forward power) and buck mode (reverse power). When d is more than 1 or φ is positive, the converter works in boost mode. When d is less than 1 or φ is negative, the converter works in buck mode. The losses of the DAB converter are composed of the condition loss, switching loss and core loss.

System Integration: The system integration of HEVs consists mainly of PL, PS, SS, Supervisory Control System (SCS) and Start Stop System. The structure of the series HEV powertrain is given in Fig. 2.

C. Driving Cycle

Driving cycle is the relationship of the speed versus time for vehicles. WLTP is a single driving cycle including four stages, low speed (WL-L), medium speed (WL-M), high speed (WL-H) and extra high speed (WL-E). WLTP is applied in this paper. Multiple iterations for driving cycles can keep the fuel consumption reasonable and balanced for the different driving cycles.

D. Equivalent Fuel Consumption

For evaluation of fuel economy, the most suitable approach is converting the consumed charge and fuel into EFC. EFC is essential which can evaluate control strategies, especially for tuning process of variables. The less EFC is, the better performance has control strategy. The EFC is defined as:

$$M_{efc}=M_f+S_{d,efc} \times \Delta SOC \times Q_{max} \times v_{b,OC},\ \Delta SOC>0 \tag{4}$$

$$M_{efc}=M_f+S_{c,efc} \times \Delta SOC \times Q_{max} \times v_{b,OC},\ \Delta SOC<0 \tag{5}$$

M_{efc} and M_f represent the mass of EFC and fuel consumption respectively. Q_{max} represents the maximum capacity of the battery. $v_{b,OC}$ represents open circuit battery voltage. SOC represents state of charge. $\Delta SOC=SOC_{initial}-SOC_{final}$. $S_{d,efc}$ and $S_{c,efc}$ represent parameters related to driving cycles. The fuel energy E_f and electrical energy E_e are defined as:

$$E_f = m_f Q_{LHV} \tag{6}$$

$$E_e = \Delta SOC Q_{max} v_{b,OC} \tag{7}$$

Q_{LHV} represents the lower heating value of the fuel. m_f represents the accumulated fuel consumption. The range of SOC is [50%, 80%]. The summed fuel economy of WL-E is much more heavy than other drive cycles, so half EFC of WL-E will be considered for total fuel economy. The definition of total EFC is defined as [14]:

$$M_{tot}=M_{efc,WL-L}+M_{efc,WL-M}+M_{efc,WL-H}+M_{efc,WL-E}/2 \tag{8}$$

E. Other

This paper mainly focuses on the control of the powertrain, so the accurate series HEV model with powertrain and car response is necessary. The series HEV model in the paper was modified based on the model built by Dr. Wassif Shabbir. European family saloon is representative and suitable, so it is applied for the model [10].

This rest of the paper is organized as follows: Section II presents TCS、DC-link voltage control and the combined control strategy. In Section III, a series of simulations on series HEV model are conducted and analysis is made according to simulation results. Conclusions are summarized in Section IV.

II. CONTROL STRATEGIES

A. Thermostat Control Strategy

In 1995, Petit and Anderson designed basic knowledge of control strategies for series HEV and TCS [15]. In 1996, Hochgrafe *et al*. studied more knowledge on TCS [16]. Nowadays, the rule of TCS is more complete and become a simple, basic and traditional control strategy for series HEV [17]. The relationship of PS and SS is as follows,

$$P_{PS,cop}+P_{SS}=P_{PL}, \tag{9}$$

$P_{PS,cop}$ is PS operation power which should be set and is usually the most power efficient point of PS operation. The value of $P_{PS,cop}$ should be selected according to the mass of EFC. The detailed principle of TCS is: SOC is more than 80%, PS stops to run and SS starts to discharge; SOC is less than 50%, PS starts to run; SOC is more than 50% and less than 80%, PS keeps the previous state.

The TCS rule diagram about SOC and P_{PL} is shown in Fig. 3. S represents the state of PS: S=1 means that PS runs and S=0 means that PS stops to run.

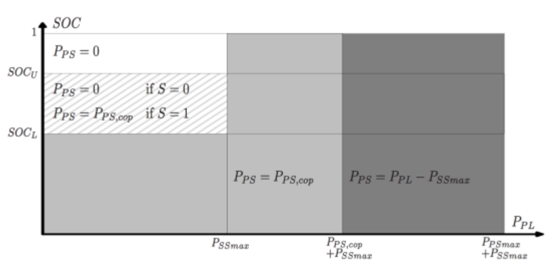

Fig. 3. The diagram of TCS rule

B. DC-Link Voltage Control Strategy

The block of DC-link voltage control is a part of the DAB converter. Constant voltage PI control (CVPI) and persistent zero voltage switching control (PZVS) are two types of DC-link voltage control strategies.

1) Constant voltage PI control: The block diagram of CVPI control is shown in Fig. 4. The input of CVPI control is the error between the reference voltage and real-time voltage of DC-link, while the output is real-time voltage of DC-link. The reference voltage of the DC-link is designed as 700 V. Thus, the voltage of the DC-link tends to be controlled as 700

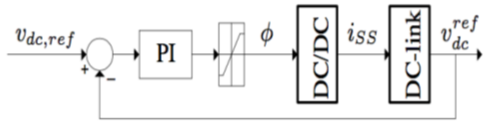

Fig. 4. The block diagram of CVPI control

V by PI control and the voltage should keep a steady state. The control principle is that the power of DAB converter is

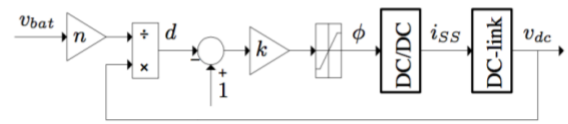

Fig. 5. The block diagram of PZVS control

controlled by value of φ. The parameters of PI control are set: K_i = 0.016 and K_p = 0.16.

2) Persistent Zero Voltage Switching Control: The block diagram of PZVS control is shown in Fig. 5 [13]. From the diagram, the relationship of d and φ is: φ = K (1 – d). K represents a constant parameter, and the condition that K should satisfy is: $-\frac{2}{\pi}\leq\frac{1}{k}\leq\frac{2}{\pi}$. Thus, $K\geq\frac{2}{\pi}$ [13].

Because of the relationship between DAB power flow and DC-link voltage, operating points in the Forward-Buck and Reverse- Boost regions tend towards the point (φ, d) = (0, 1), yielding a stable controller [13]. This is because the operation points in the reverse-boost and forward-buck regions naturally tend towards the origin. Selecting value of K is an essential part to minimum the mass of fuel economy.

C. The Combined Control Strategy

TCS is a traditional control strategy and DC-link control strategy is a new control strategy for series HEV, which both have good control effects on vehicle driving. Thus, it is possible that a new control strategy has a better performance by combining them. The block of supervisory controller is independent of the block of PL, PS, SS and DC-link in the series HEV model. Some components are added in $V_{dc,ref}$ and added between V_{bat} and V_{dc} according to Fig. 4 and Fig. 5 on the model under TCS.

1) Tuning Parameters: The key point of the paper is applying TCS and DC link voltage control strategies together to achieve the better performance compared with individual control strategy.

K is the tuning parameter for PZVS. φ = K (1 − d). φ is a controlled variable for PZVS and CVPI. The control law corresponds to a diagonal line passing through the origin (d, φ) = (1, 0) on the d-φ plane [18]. When K is tuned, diagonal line of d-φ is bended to pass through the region of best efficiency.

$P_{PS,cop}$ is the only tuning variable for TCS. By tuning, the value of $P_{PS,cop}$ will make PS run at optimal operating point. An objective tuning process should be conducted to fix the accurate value of K.

2) Tuning Process: Model simulations were conducted on all combinations of drive cycles, PZVS, and TCS. The simulations have been used to iteratively tune K and $P_{PS,cop}$ by a simple search method to minimizeM_{efc}.

For tuning K, model simulations were conducted with four drive cycles individually under TCS with different K values. By obtaining minimum M_{efc}, the corresponding optimal K will be found individually for four driving cycles of WLTP. Based on calculation equation of total M_{efc}, the least value of M_{efc} will be found, so the optimal K for WLTP will be obtained.

For tuning $P_{PS,cop}$ (TCS), model simulations were conducted with four drive cycles individually under TCS with different $P_{PS,cop}$ values and fixed value of K. By obtaining minimum M_{efc}, the corresponding optimal $P_{PS,cop}$ will be found individually for four driving cycles of WLTP. The next step is to calculate the total M_{efc} and find the minimum value of M_{efc}. Then the optimal value of $P_{PS,cop}$ will be obtained.

The appropriate range of K is selected as [2, 5]. The values of $P_{PS,cop}$ (TCS) is fixed in the process of tuning K. For TCS, based on the calculation rules of total M_{efc} in the whole driving cycle, K equals 5 when the total M_{efc} is minimum. Thus, 5 is the optimal value of K for TCS.

The tuning range of $P_{PS,cop}$ is [16, 28] for TCS. Model simulations were conducted iteratively on all combinations of drive cycles under TCS and PZVS with different values of $P_{PS,cop}$ and K=5. The simulation result of tuning $P_{PS,cop}$ is whatever value of $P_{PS,cop}$ is, the M_{efc}s keep 0.0708 and 0.1427 with WL-L and WL-M respectively. The diagrams of M_{efc} and $P_{PS,cop}$ with WL-H and WL-E are shown in Fig. 6.

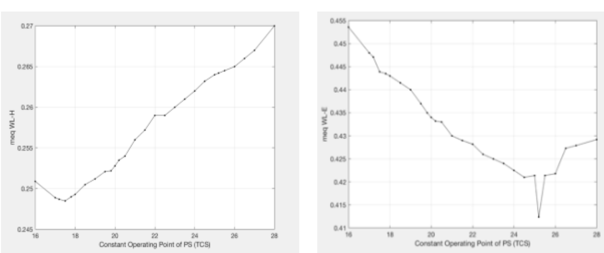

Fig. 6. The tuning diagrams of M_{efc} and $P_{PS,cop}$ with WL-H and WL-E

It can be found that when $P_{PS,cop}$ equals 17.5 and 25.2, M_{efc}s are least with WL-H and WL-E respectively. The total M_{efc} is sum of M_{efc} for four stages. The total M_{efc} is minimum when $P_{PS,cop}$ is 19.8. Thus, the tuning result of $P_{PS,cop}$ is that $P_{PS,cop}$ equals 19.8 under TCS. The tuning results are given in Table I. In conclusion, the optimal value of K and $P_{PS,cop}$ for WLTP are 5 and 19.8 respectively.

III. Simulation and Results

All of the car dynamics were built in Simulink by using the SimMechanics library. The series HEV model was

TABLE I. The Tuning Results

Control strategy	Tuning variables	M_{efc} (WL-L)	M_{efc} (WL-M)	M_{efc} (WL-H)	M_{efc} (WL-E)	Total M_{efc}
TCS	K	5	5	4.5	4.8	5
	$P_{PS,cop}$	No min	No min	17.5	25.2	19.8

the SimMechanics library. The series HEV model was running with optimal values of K and $P_{PS,cop}$ for WLTP. The results are two parts: the loci of d-φ and simulation result graphs of the power, the voltage of DC link, SOC and mass of EFC.

A. The Result of d- φ

The loci of d-φ in WL-M, WL-H and WL-E are shown in Fig. 7 and Fig. 8 respectively. The left diagrams are the results under TCS and PZVS. The right diagrams are the results under TCS and CVPI.

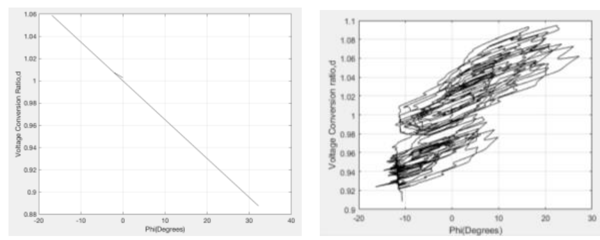

Fig. 7. The loci of d-φ under TCS-PZVS and TCS-CVPI in WL-M

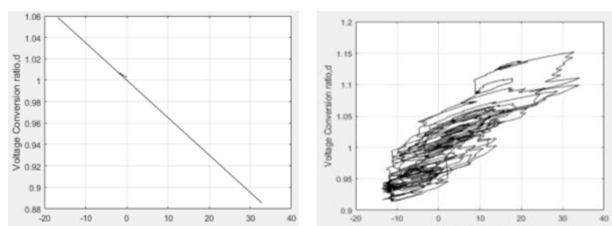

Fig. 8. The loci of d-φ under TCS-PZVS and TCS-CVPI in WL- H

For PZVS, the ranges of φ and d are [-17, 33] and [0.88, 1.06] respectively. For CVPI, the ranges of φ and d are [-17, 35] and [0.9, 1.1] respectively. The loci of d-φ extend more into quadrant of positive φ. The reason is that the magnitudes of positive power are more than magnitudes of positive power for SS.

The loci of PZVS are straight lines passing through (0,1) and its slope is -1/K. Simulation results under CVPI are the loci of d-φ passing around (0,1) and with a positive slope. The straight line loci under PZVS passes through (0,1). When φ changes its sign, these lines of PZVS avoid the low efficiency regions at $d \neq 1$. For CVPI, the converter is often operated at inefficient points around the (0,1) [1]. As the stages speeds of WLTP increasing, maximums of φ and d for CVPI increase.

B. The Results of Other Variables

For each stage of driving cycle, simulation is conducted for two times, which benefits to show the performance of control strategy. The simulation results under TCS and DC-link voltage control for WL-L are shown at Fig. 9.

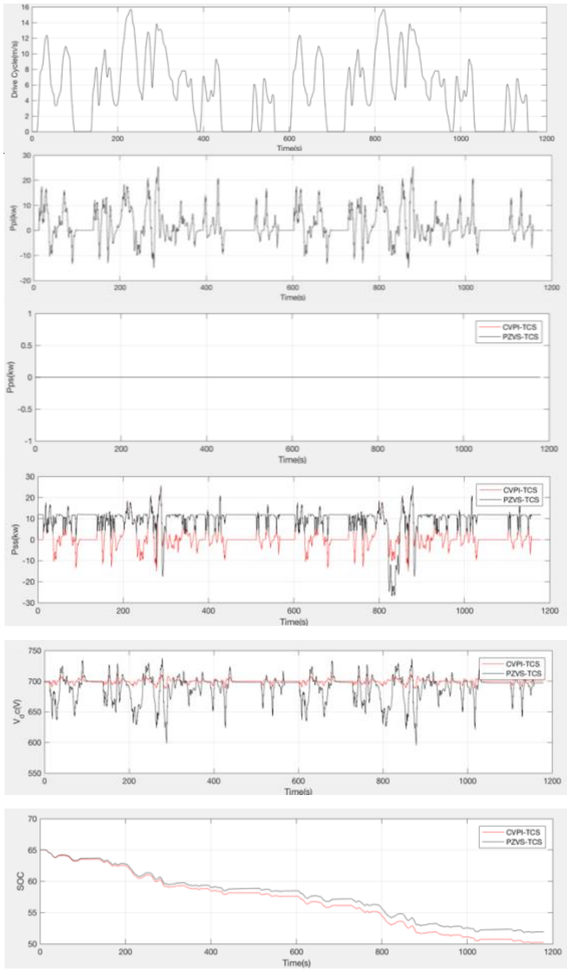

Fig. 9. The simulation results with WL-L

The power of PL only depends on road load. It means that road load is dependent on driving cycle. Thus, the time histories of PL power are unchangeable whatever the control strategy is. When the speed of series HEV increases, the power of PL is positive and there is a power spike. When the speed of vehicle decreases, the power of PL is negative and that means the vehicle is braking. The DC-link voltage under CVPI is more stable than the DC-link voltage under PZVS as the PI control.

It can be found that there is a correlation between the power of SS and the voltage of DC-link under PZVS. The voltage of DC-link drops when the power of SS increases over zero; the voltage of DC-link increases when the power of SS drops below zero. This imposes an almost linear and with negative slope dependence of the respective phase-shift variable to V_{dc}, since variation of V_{bat} is small. The mass of EFC under PZVS is less than the mass of EFC under CVPI. The mass of EFC under PZVS and TCS performs better than the individual control scheme.

For WL-L, the maximum power of PL is about 25kW, while the minimum power of PL is -15 kW. For WL-L, the average speed is low, so the demanded power of PL is low. SS mainly supplies for PL, and PS does not run. The DC link voltage are around 700V as $V_{dc,ref}$ =700 V. The simulation results under TCS scheme and DC-link voltage control for WL-M ,WL-H and WL-E are shown at Fig. 10 and 11.

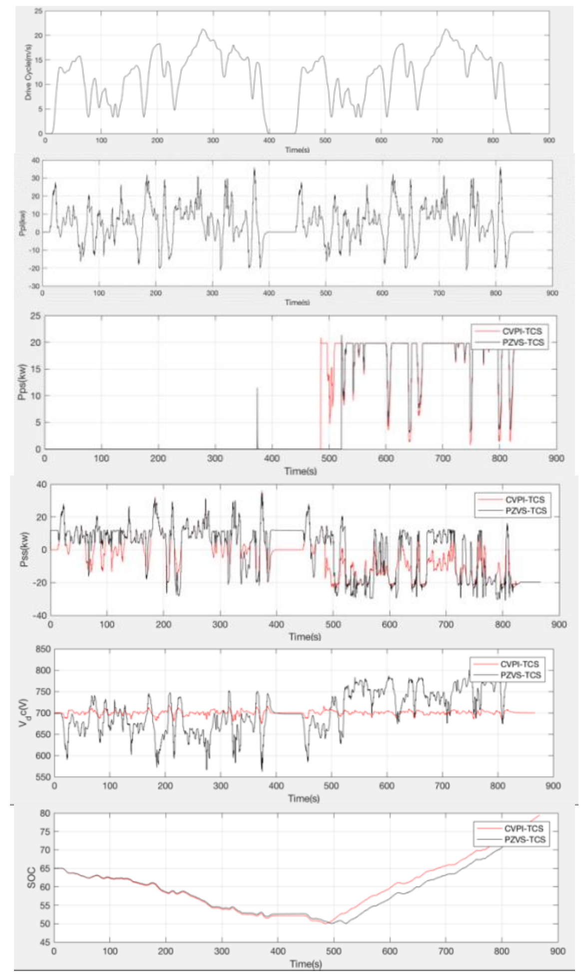

Fig. 10. The simulation results with WL-M

With WL-M, the power range of PL extends because the average speed of vehicle increases compared with WL-L. When SOC under TCS drops to 50% at the time 500 s, the PS starts to run and the battery is being charged. For TCS, M_{efc} under PZVS falls by 3.8% compared with CVPI for WL-M.

With WL-H, the period that the powers of PS keep 0 at the beginning for WL-H becomes shorter than the period of WL-M. The reason is that the demanded load power of PL exceeds the power of the battery, so the PS and SS work together to power the motor. For TCS, M_{efc} under PZVS falls by 6.16% compared with CVPI for WL-H. For WL-E, the maximum power of PL is about 50kW, while the minimum power of PL is -20 kW. The load power of PL has the highest demand of power, and the PS is continuously switched on as the power of SS is lower than the demand load power. For

TCS, M_{efc} under PZVS falls by 5.32% compared with CVPI for WL-E. The results of M_{efc} are given in Table II.

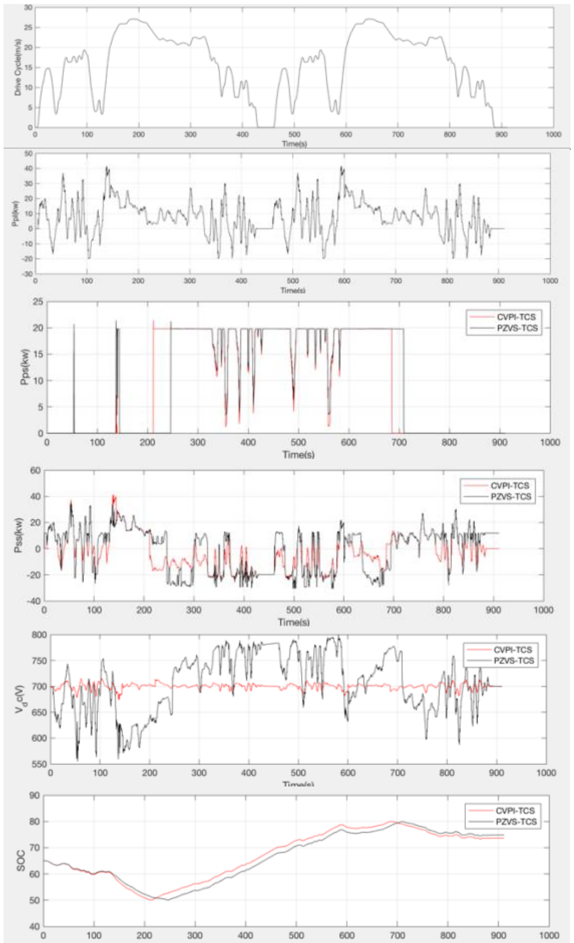

Fig. 11. The simulation results with WL-H

TABLE II. THE RESULTS OF M_{EFC}

Stages	WL-L		WL-M		WL-H		WL-E	
Combine	TCS-CVPI	TCS-PZVS	TCS-CVPI	TCS-PZVS	TCS-CVPI	TCS-PZVS	TCS-CVPI	TCS-PZVS
M_{efc}	0.0800	0.0708	0.1484	0.1427	0.2648	0.2485	0.4451	0.4214

IV. CONCLUSION

TCS and DC-link voltage control are combined to improve fuel economy in the paper. By tuning a parameter under DC-link voltage control and a selected constant under TCS, the points of minimum mass of equivalent fuel consumption are marked for WLTP driving cycle. By tuning of two important control variables, the scheme of PZVS outperforms the scheme of CVPI in terms of the mass of equivalent fuel consumption. The improvements are achieved for four stages of WLTP driving cycle. Total mass of equivalent fuel consumption of PZVS falls by 4.62% compared with CVPI and TCS for WLTP. Tuning variables of DC-link voltage and TCS is effective method to improve the fuel consumption. After simulations and analysis, this scheme proves very effective for series HEVs in an urban environment.

REFERENCES

[1] I. Reşitoğlu , K. Altinişik , A. Keskin, “The pollutant emissions from diesel-engine vehicles and exhaust aftertreatment systems,” Clean Technologies & Environmental Policy, vol.17, pp.15-27, 2015.

[2] F. Y. Wang, “Agent-based control for networked traffic management systems. IEEE Intelligent Systems,” vol.20, pp.92-96, 2005.

[3] H. Y. Guo, L. H. Song, J. Liu, F. Y. Wang, D. P. Cao, H. Chen, C. Lv, P. K. Luk, “Hazard-evaluation-oriented moving horizon parallel steering control for driver-automation collaboration during automated driving,” Journal of Automatica Sinica,” vol.5, pp.1062-1073, 2018.

[4] L. Li, X. Y. Peng, F. Y. Wang, D. P. Cao, L. X. Li, “A situation aware collision avoidance strategy for car-following,” Journal of Automatica Sinica, vol.5, pp.1012−1016, 2018.

[5] Y. Xing, C. Lv, L. Chen, D. J. Wang, H. Wang, D. P. Cao, E, Velenis, F. Y. Wang, “Advances in vision-based lane detection: algorithms, integration, assessment, and perspectives on ACP-based parallel vision.,” Journal of Automatica Sinica, vol.5, pp.645-661, 2018.

[6] Q. Zhou, F. Y. Wang, “Driver assisted fuzzy control of yaw dynamics for 4WD vehicles”, Intelligent Vehicles Symposium IEEE, 2004, pp.425-430.

[7] L. Li, Y. S. Lv, F. Y. Wang, “Traffic Signal Timing via Deep Reinforcement Learning,” Journal of Automatica Sinica, vol.3, pp.247-254, 2016.

[8] Y. Xing, C. Lv, Z. Z. Zhang, H. J. Wang, X. X. Na, D. P. Cao, V. Efstathios, F. Y. Wang, “Identification and Analysis of Driver Postures for In-Vehicle Driving Activities and Secondary Tasks Recognition,” IEEE Transactions on Computational Social Systems, vol.5,pp.95-108, 2018.

[9] X. Wang, X. H. Zheng, Q. P. Zhang, T. Wang, D. Y. Shen, “Crowdsourcing in ITS：The State of the Work and the Networking,” IEEE Transactions on Intelligent Transportation Systems, vol.17, pp.1596 -1605, 2016.

[10] S. A. Evangelou, W. Shabbir, “Dynamic modeling platform for series hybrid electric vehicles,” Ifac Papersonline, vol.49, pp.533-540, 2016.

[11] D. Graovac, M. Purschel, “IGBT power losses calculations using data-sheet parameters,” Infineon Technologies, 2009.

[12] M. H. Bierhoff, F. W. Fuchs, “Semiconductor losses in voltage source and current source IGBT converters based on analytical derivation,” Power Electronics Specialists Conference IEEE, vol.4, pp.2836-2842, 2004.

[13] M. Roche, W. Shabbir, S. A. Evangelou, “Voltage control for enhanced power electronic efficiency in series hybrid electric vehicles,” IEEE Transactions on Vehicular Technology, vol.66, pp.3645-3658, 2017.

[14] S. Wassif, “Control strategies for series hybrid electric vehicles,”Ph.D dissertation, Imperial College London, London, 2015.

[15] C. Anderson, E. Pettit, “The effects of APU characteristics on the design of hybrid control strategies for hybrid electric vehicles,” Braking Systems, 1995.

[16] C. G. Hochgraf, M. J. Ryan, H. L. Wiegman, “Engine control strategy for a series hybrid electric vehicle incorporating load-leveling and computer controlled energy management,” 1996.

[17] R. Johri, Z. Filipi, “Optimal energy management of a series hybrid vehicle with combined fuel economy and low-emission objectives,” Proceedings of the Institution of Mechanical Engineers Part D Journal of Automobile Engineering, vol.228, pp.1424-1439, 2014.

[18] S. A. Evangelou, M. A, R. Shaikh, “Hybrid electric vehicle fuel minimization by DC-DC converter dual-phase-shift control,” Control Engineering Practice, vol.64, pp.44-60, 2017.